

## Improvement of sewage sludge dewaterability and immobilization of the heavy metals by using pretreated steel slag

Sha Wan<sup>a</sup>, Yi Han<sup>b,\*</sup>, Min Zhou<sup>a</sup>, Xian Zhou<sup>c</sup>, Yuchi Chen<sup>a</sup>, Yiqie Dong<sup>a</sup>, Fucai Huang<sup>a</sup>, Teng Luo<sup>a</sup>, Yun Zheng<sup>c</sup>, Haobo Hou<sup>a,\*</sup>

<sup>a</sup>School of Resource and Environmental Science, Wuhan University, Wuhan, Hubei 430072, China, Tel. +86 13908644407; emails: 18607217399@163.com (H. Hou), wansha@whu.edu.cn (S. Wan), zhomin@whu.edu.cn (M. Zhou), 396075932@qq.com (Y. Chen), 861883943@qq.com (Y. Dong), 374136191@qq.com (F. Huang), 1304707801@qq.com (T. Luo)

<sup>b</sup>College of Resources and Environment, Anqing Normal University, Anhui 246011, China, Tel. +86 13971647463; email: 952635963@qq.com

<sup>c</sup>Key Laboratory of Geotechnical Mechanics and Engineering of Ministry of Water Resources, Yangtze River Scientific Research Institute, Wuhan, Hubei, 430010, China, emails: zhouxian@whu.edu.cn (X. Zhou), 18995600830@163.com (Y. Zheng)

Received 4 May 2019; Accepted 8 November 2019

### ABSTRACT

Pretreated steel slag was used to enhance sludge dewatering and the potential risk posed by heavy metals (HMs) was discussed in this study. Specific resistance to filtration and capillary suction time decreased by 98.8% and 78.6%, respectively, when 40 mg/g of dry sludge steel slag were added. The zeta potential showed that the steel slag addition considerably affected sludge with small particle. New fluorescence peaks indicated that the extracellular polymeric substance (EPS) structure was damaged and partially dissolved into solution EPS (S-EPS). The floc surface charge was reduced, and the small particles were enlarged owing to the flocculation of a small amount of S-EPS. Microstructure analysis showed that the inorganic components in the steel slag provided skeletal support during mechanical dewatering and ensured the outlet channel. Analysis of the HMs indicated that the Cu and Mn concentrations decreased by 60% and 85.2% in the liquid phase, respectively, and the Zn concentration increased 2.2 times. Moreover, the results of the toxicity characteristic leaching procedure showed that the Cu, Mn, and Zn concentrations in the sludge cakes decreased by 93.5%, 27.1%, and 22.1%, respectively. Therefore, the addition of steel slag reduced the risk and enhanced the immobilization of HMs.

*Keywords:* Sewage sludge; Dewatering; Steel slag; Heavy metals; Particle size

### 1. Introduction

Sludge treatment and disposal are urgent environmental problems in various countries. In China, more than 9.2 million tons of dry sewage sludge were produced in 2017 [1]. In Europe, the annual production of dry sewage sludge is estimated to exceed 10 million tons in 2020 [2]. Wastewater treatment plants are facing huge challenges with regard

to the management of waste activated sludge owing to its increased production. The water content of sludge generally ranges from 95% to 99%, and reaches 75%–80% even after mechanical dewatering [3]. Therefore, dewatering is a key process in sludge volume reduction, transport, and ultimate disposal. Various methods, such as ultrasonication, thermal treatment, oxidation, flocculence, electro-dewatering, freezing, and thawing, have been developed to improve sludge

\* Corresponding author.

dewaterability [4–10]. Extracellular polymers are important in the bioflocculation, settling, and dewatering of activated sludge. Extracellular polymeric substance (EPS), which is a polymer secreted by microorganisms during the metabolic process, surrounds the cell wall in a certain environment. The components of EPS include several polymers, such as protein, polysaccharide, nucleic acid, and humic acid [11]. Yu et al. [12] analyzed the structure and distribution of EPS and found that it is composed of supernatants, slime, loosely bound EPS, tightly bound EPS, and pellets. The zeta potential is highly related to extracellular polymers, and a strong correlation between specific resistance to filtration (SRF) and the zeta potential has been demonstrated in a previous study [13]. Moreover, the oxidation–reduction potential is positively correlated to SRF ( $r = 0.89, p < 0.05$ ) [14]. Physical conditioners or skeletal builders such as gypsum [15], red mud [16], cement [17], lignite, and polyelectrolytes [18] have been utilized to enhance sludge dewaterability because they can decrease sludge compressibility and provide a flow channel for free water.

Steel slag is a major byproduct of steel production. More than 100 million tons of steel slag are discharged in China annually [19]. European and other developed countries utilize up to 70%–80% of the slag they generate, whereas slag utilization in China is only 22% [20]. In the past decade, steel slag has been used to remove phosphate [21] and dyes [22] from contaminated water. Steel slag-based materials can also be effectively used for sludge stabilization [23]. However, studies on steel slag that focus on improving the dewatering performance of sludge in conditioning are rare. The chemical composition of steel slag varies with the mineral composition of raw materials, such as iron ore and limestone, and f-CaO is the main mineral phase in steel slag.

Raw sewage sludge (RS) is conditioned with pretreated steel slag in this study, and samples are measured for SRF and capillary suction time (CST). The zeta potential, particle size distribution, and 3D fluorescence of the conditioned sludge are examined to reveal possible mechanisms. The sludge cake produced after conditioning typically contains pollutants such as pathogens, organic matter dioxins, and heavy metals (HMs), which pose a potential risk to the ecological system and human health [24]. Therefore, the contents

of HMs in the filtrate and leaching liquid of sludge cake are measured, and the chemical species distribution of HMs is analyzed.

## 2. Materials and methods

### 2.1. Raw sludge

The RS used in this study was a mixture of primary and secondary sludge from the Sanjintan Sewage Treatment Plant in Wuhan, China. The capacity of this municipal wastewater treatment plant is  $3 \times 10^5$  m<sup>3</sup>/d. The RS samples were collected in polypropylene containers and stored at 4°C in a refrigerator, and the preservation period should not exceed 4 d [8]. Before the experiment, the RS was removed from the refrigerator and placed in environmental conditions until the temperature reached 20°C. The characteristics of the sludge samples were evaluated using standard methods (US Environmental Protection Agency [EPA], 1995). The results are shown in Table 1.

### 2.2. Total metal concentrations and toxicity characteristic leaching procedure

Table 2 shows that the total content of Cu and Zn in the RS exceeded the limit values of the Environmental Quality Standard for Soils (GB15618–1995, PR China, 1995). Thus, the RS posed potential risks to the environment. Moreover, the total content of Mn was high. However, no limit exists for total Mn content in the soil standard. Aschner et al. [25] reported that Mn causes strong neurotoxicity in the human body. Therefore, the environmental risks posed by Cu, Zn, and Mn were investigated in this study.

Table 1  
Basic characteristics of raw sludge

Parameters	Moisture (%)	pH	Organic content (%)	CST(s)
RS	79.3 ± 2.8	7.18 ± 0.14	40.45 ± 0.21	412 ± 4.5

Table 2  
Total content and leaching value of HMs in RS (Mean ± SD,  $n = 3$ )

	Total content (mg/kg)		TCLP leaching (mg/L)		
	RS	Limit value <sup>a</sup>	RS	Limit value <sup>b</sup>	Limit value <sup>c</sup>
Cr	83 ± 5	90	0.14 ± 0.001	1.5	4.5
Cu	127 ± 4	35	0.52 ± 0.018	0.5	40
Mn	523 ± 18	/	13.92 ± 1.017	2	100
Ni	39 ± 2	40	N.d	1	0.5
Pb	30 ± 4	35	N.d	1	0.25
Zn	503 ± 12	100	10.48 ± 0.111	2	100

N.d = Not detected.

<sup>a</sup>Environmental Quality Standard for Soils (first-level standard), GB15618–1995, PR China.

<sup>b</sup>Integrated Wastewater Discharge Standard, GB8978–2002, PR China.

<sup>c</sup>Standard for Pollution Control on the Landfill Site of Municipal Solid Waste, GB 16889–2008, PR China.

Leachability is another important parameter for assessing the toxicity and bioavailability of HMs in sludge. The US EPA's Toxicity Characteristic Leaching Procedure (TCLP) (TCLP, USEPA, 1997) was applied in this study [26].

The leaching concentrations of Mn, Zn, and Cu exceeded the limit values of the Integrated Wastewater Discharge Standard (GB8978–2002, PR China). In this study, TCLP leaching concentrations were used to assess the environmental risks of Mn, Zn, and Cu.

### 2.3. Pretreatment of steel slag

The steel slag was obtained from the Wuhan Iron and Steel Corporation in China. It was crushed to particles smaller than 80  $\mu\text{m}$  by grinding in a laboratory ball mill for 30 min. The main chemical compositions are listed in Table 3.  $\text{MgO}$ ,  $\text{Al}_2\text{O}_3$ ,  $\text{SiO}_2$ ,  $\text{CaO}$ , and  $\text{Fe}_2\text{O}_3$  were the main mineral phases found in the steel slag.

The morphological features of the steel slag treated through ball milling are shown in Fig. 1. The steel slag was powdery and resembled cement after being ground and sifted. Numerous fine particles appeared and their outline was an irregular polyhedron.

The sieved steel slag was examined using a laser particle size analyzer. As shown in Fig. 2., the proportion of particles smaller than 20  $\mu\text{m}$  exceeded 60%, and the proportion of particles smaller than 40  $\mu\text{m}$  was approximately 90%. The steel slag achieved small particle sizes and a large specific surface area after grinding, which were conducive to rapid dispersion in sludge.

### 2.4. Experimental procedure

The RS was rapidly stirred for 30 min to ensure that the sludge particles were evenly mixed with water. Experiments were conducted in a glass reactor equipped with a thermometer and an electric stirrer. In each experiment, 10, 20, 30, 40, 50, 60, and 70 mg/g of dry sludge (DS) steel slag powder was added to 500 mL of the pretreated sludge (the dosage was calculated on the basis of dry solid content). The sludge was conditioned with steel slag at 300 rpm for 5 min and at 100 rpm for 5 min. The sample was subsequently analyzed.

### 2.5. 3D excitation–emission matrix (EEM)

EEM spectra are a collection of emission spectra over a range of excitation wavelengths and can be used to identify fluorescent compounds present in complex mixtures. The peak locations, peak intensities, and ratios of different peaks in the EEM spectra of the EPS samples were not substantially influenced by ionic strength. 3D EEM spectra were measured with a Hitachi F-4500 fluorescence spectrophotometer with excitation and emission ranges of 200–400 nm and 220–550 nm, respectively, at 5 nm sampling intervals. The spectra were recorded at a scan rate of 12,000 nm/min using excitation and emission slit bandwidths of 3 nm. Each scan exhibited 67 emission and 41 excitation wavelengths. Origin 8.0 (OriginLab Inc., USA) was used to process the EEM data.

Table 3  
Main inorganic chemical compositions of raw sludge and steel slag (wt%)

Constituents	MgO	$\text{Al}_2\text{O}_3$	$\text{SiO}_2$	$\text{P}_2\text{O}_5$	$\text{SO}_3$	CaO	$\text{K}_2\text{O}$	$\text{Fe}_2\text{O}_3$
RS	1.42	11.04	30.73	5.12	1.95	3.62	1.69	10.97
Steel slag	5.28	3.19	18.67	1.26	0.53	40.77	1.37	12.01

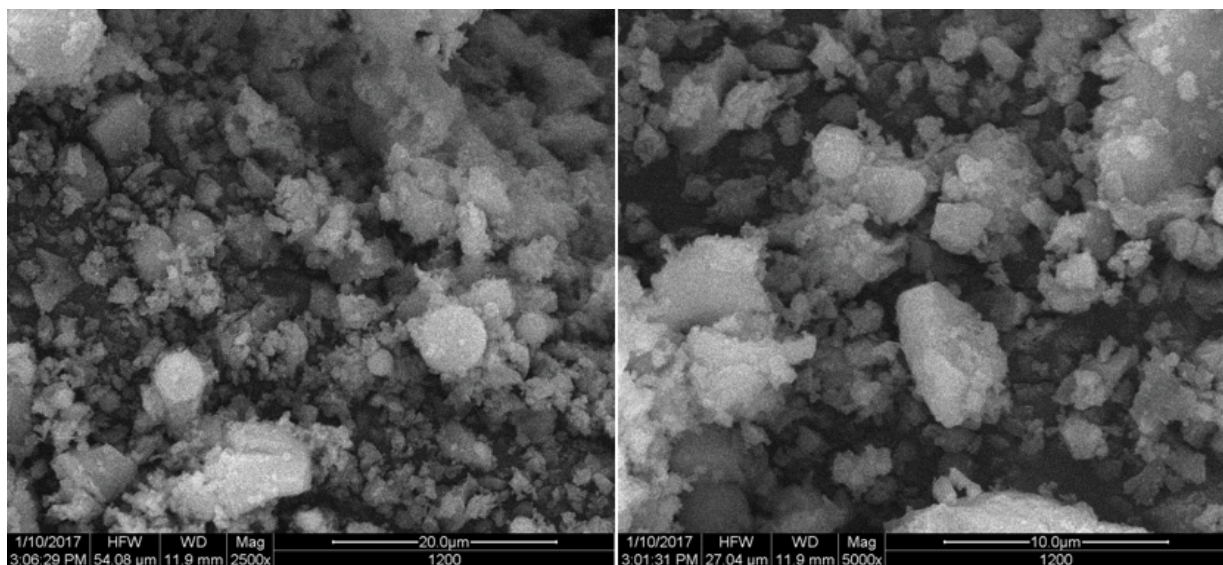


Fig. 1. SEM of steel slag.

### 2.6. Analysis of other items

SRF is an essential indicator of sludge dewatering performance and has been described in previous studies [27,28]. CST was measured with a 304M CST equipment (Triton, UK) at 25°C. A sufficient amount of sludge was poured into a funnel with a 1.8 cm inner diameter, and the time was recorded automatically. The zeta potential was determined with a Malvern Zetasizer Nano ZS (Malvern Instruments Ltd., UK) by collecting the supernatant of the sludge after centrifugation at 4,500 rpm for 5 min. The supernatant was then mixed with the sludge at a ratio of 9:1. Particle size distribution was determined with a Mastersizer 2000 laser particle size analyzer (Malvern, UK) at a stirring rate of 1,000 rpm after the sludge was dispersed in an aqueous solution. The chemical speciation of HMs was conducted using the Tessier sequential extraction procedure [29]. Each test was conducted in triplicate, and the results were expressed as mean values  $\pm$  SD.

## 3. Results and discussion

### 3.1. Sludge dewaterability

As shown in Fig. 3, CST and SRF values remarkably decreased with increased slag dosage. Moreover, CST and SRF curves considerably decreased as dosage increased from 0 to 20 mg/g DS. The curves slowly decreased when the dosage exceeded 30 mg/g DS. The changes in CST and SRF were small when the dosage was more than 50 mg/g DS. The water content of the mud cake decreased with increased steel slag dosage (Fig. 4). In addition, the moisture content of mud cake decreased when steel slag dosage exceeded 20 mg/g DS. In general, the dewatering performance of sludge can be remarkably improved when the dosage of steel slag exceeds 20 mg/g DS. However, steel slag is an inorganic material, and several of its components are difficult to dissolve in water. Excessive steel slag dosage will increase the dry base of sludge and the treatment cost. This analysis showed that steel slag dosage of 20–50 mg/g DS was suitable.

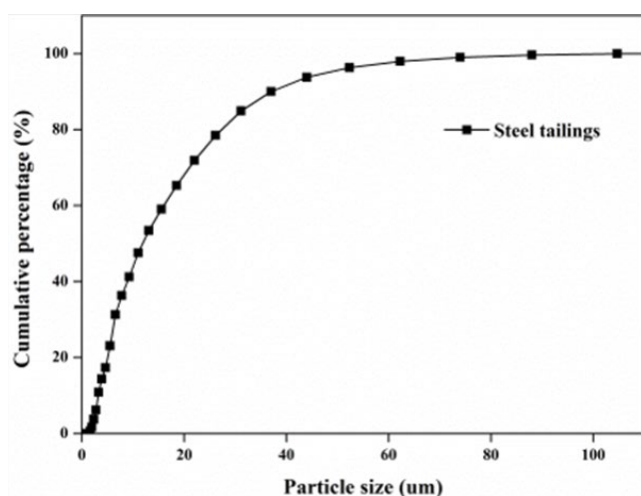


Fig. 2. Particle size distribution evolution.

### 3.2. Possible mechanism of improved sludge dewaterability

A particle size classification method reported in a previous study [30] was used to investigate the mechanism of the steel slag in improving sludge dewatering performance. RS passed through 0.5, 0.25, 0.1, and 0.075 mm sieves was denoted as  $S_1$ ,  $S_2$ ,  $S_3$ , and  $S_4$ , respectively. The characteristics of the sludge samples are shown in Table 4. In accordance with the abovementioned experimental results, 40 mg/g DS steel slag was used in the subsequent experiment. The mechanism of the steel slag in improving sludge dewatering performance was evaluated with the addition of steel slag to pretreated samples combined with zeta potential, particle size distribution, 3D fluorescence spectrum, and SEM analysis.

The results in Table 4 show that the moisture content and pH values of the samples after grading and the content of organic matter decreased because large particles of fibers and domestic refuse were trapped in the sludge during grading. Table 5 demonstrates that the chemical composition of the

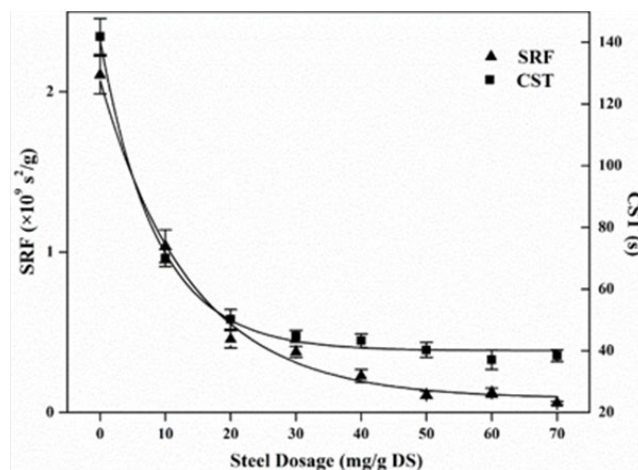


Fig. 3. SRF and CST evolution of sludge as a function of steel dosage.

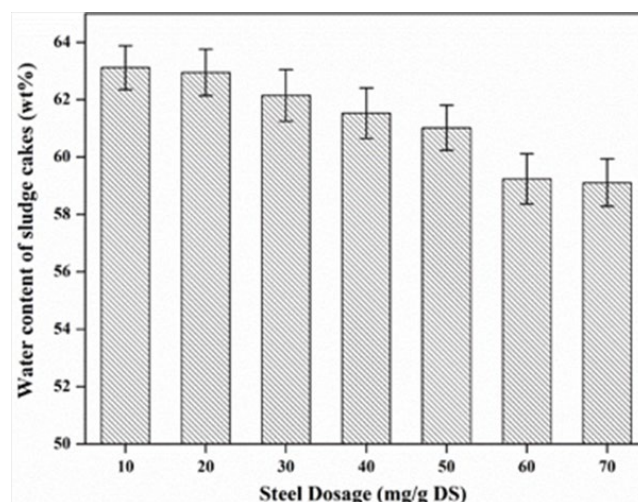


Fig. 4. Water content of sludge cake evolution as a function of steel dosage.

Table 4  
Basic characteristics of the sludge samples

Parameter	Value		
	RS	S <sub>2</sub>	S <sub>4</sub>
Moisture (%)	95.02	95.11	96.50
pH	7.18 ± 0.14	7.20 ± 0.11	7.21 ± 0.10
Organic content (%)	39.10 ± 0.31	36.07 ± 0.25	35.18 ± 0.22
CST(s)	141.9 ± 7.8	148.7 ± 9.3	359.1 ± 9.8

sludge changed slightly after grading, and inorganic silicon content in sample S<sub>4</sub> (with the smallest particle sizes) increased slightly. This change was consistent with that in organic matter content. In general, the physical and chemical properties as well as the composition of the samples changed only slightly after grading.

### 3.2.1. CST analysis

The enhancement of steel slag dewaterability was assessed through the CST/zeta potential reduction percentage  $R$  (%), which is calculated as follows:

$$R_c(\%) = \frac{CST_0 - CST_e}{CST_0} \times 100\% \quad (1)$$

$$R_z(\%) = \frac{Zeta_0 - Zeta_e}{Zeta_0} \times 100\% \quad (2)$$

where  $CST_0$  is the CST of the RS (s),  $CST_e$  is the CST of the sample after conditioning (s),  $Zeta_0$  is the zeta potential of the RS (mV), and  $Zeta_e$  is the zeta potential of the sample after conditioning (mV).

The dewatering performance of the sludge samples with different particle sizes improved remarkably with the addition of the steel slag modifier. As shown in Fig. 5, the CST value remarkably decreased. The CST value increased with the decrease in particle size. However, the smaller the particle size of the experimental group, the greater the CST reduction rate. The addition of the steel slag modifier noticeably affected the sludge with small particle sizes.

### 3.2.2. Effect of zeta potential on dewaterability

The zeta potential of each experimental group considerably decreased with the addition of the steel slag modifier (Fig. 6). However, the reduction rate differed with particle size. The reduction rate of the zeta potential increased with decreased particle size, and this finding was contrary to the

situation in ferric chloride conditioning. The effect of the steel slag addition on the sludge with small particle sizes was remarkable owing to the dispersive and uniform steel slag in sludge flocs with small particle sizes. This finding was consistent with the CST results. Although the zeta potential reduction rate in the S<sub>4</sub> group was slightly lower than that in the S<sub>3</sub> group, the zeta potential in the S<sub>4</sub> group reached a small value, and the continuous decrease in the potential value had no remarkable influence on sludge dehydration performance.

### 3.2.3. Variation in particle size distribution

The size distributions of sludge with different sizes after steel slag conditioning are shown in Fig. 7. Sludge sizes with different particle sizes changed slightly after conditioning. The particle sizes of S<sub>1</sub>, S<sub>2</sub>, and S<sub>3</sub> increased slightly compared with the values in the blank group, and those in the S<sub>4</sub> group increased slightly compared with the values in the blank group. Moreover, the steel slag showed no flocculation effect. The increase in sludge floc size may be due to the coagulation of particles with surface charge neutralization. In addition, several insoluble inorganic particles in the steel slag affected particle size. On the basis of the above analysis, this study concluded that the surface charge of sludge flocs was neutralized, and several particles aggregated to form large flocs, thereby reducing the adsorption capacity of the water molecules. However, the decrease in the zeta potential was related to charge neutralization and sludge EPS content. The impact of the steel slag on EPS during conditioning was investigated further.

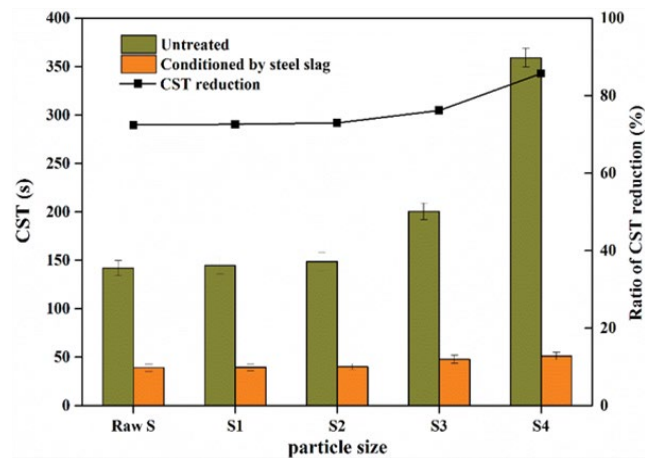


Fig. 5. CST reduction percentage evolution after steel conditioning.

Table 5  
Main inorganic chemical compositions of raw sludge sample (wt%)

Constituents	MgO	Al <sub>2</sub> O <sub>3</sub>	SiO <sub>2</sub>	P <sub>2</sub> O <sub>5</sub>	SO <sub>3</sub>	CaO	K <sub>2</sub> O	Fe <sub>2</sub> O <sub>3</sub>
RS	1.42	11.04	30.73	5.12	1.95	3.62	1.69	10.97
S <sub>2</sub>	1.48	10.98	29.93	5.61	1.99	3.78	1.73	10.97
S <sub>4</sub>	1.42	11.36	34.29	4.17	1.80	3.74	1.75	9.70

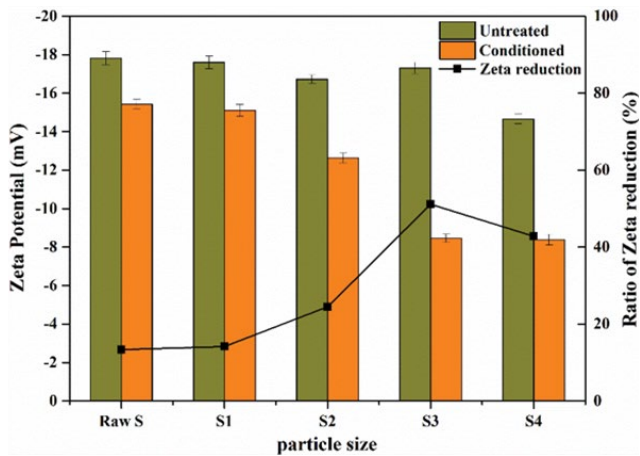


Fig. 6. Zeta potential reduction percentage evolution after steel conditioning.

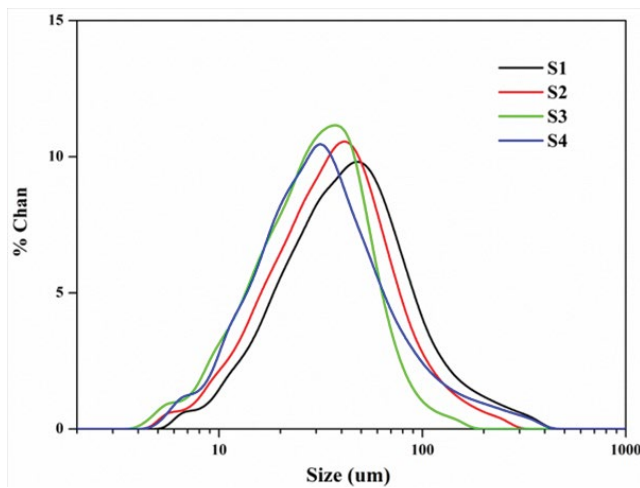


Fig. 7. Particle size distribution evolution after steel slag conditioning.

3.2.4. EEM fluorescence analysis

The 3D fluorescence spectra of the sludge samples after steel slag conditioning were obtained; the data were processed in Origin 8.0, and the findings were as follows (Fig. 8). The main peaks of the RS were located at the excitation/emission wavelengths Peak A ( $\lambda_{ex}/\lambda_{em} = 370\text{--}390/440\text{--}470$ ) and Peak B ( $\lambda_{ex}/\lambda_{em} = 340\text{--}350/435\text{--}445$ ). Peak A reflected humic acid substances [31], and Peak B was related to humic acid. Similar conclusions were obtained in studies on natural dissolved organic matter [32] and activated sludge cells [33].

New fluorescence peaks, namely, Peak C ( $\lambda_{ex}/\lambda_{em} = 280/350\text{--}360$ ) and Peak D ( $\lambda_{ex}/\lambda_{em} = 245/450$ ), appeared after steel slag pretreatment. Peak C was associated with humic acid-like fluorescence, and Peak D was a tryptophan protein-like substance [34]. The original fluorescence peak position shifted compared with the fluorescence spectra of the original sludge, and the peak intensity remarkably increased. The new fluorescence peaks indicated that the EPS structure was damaged and partially dissolved into solution EPS (S-EPS). The intensity of the main fluorescence peaks

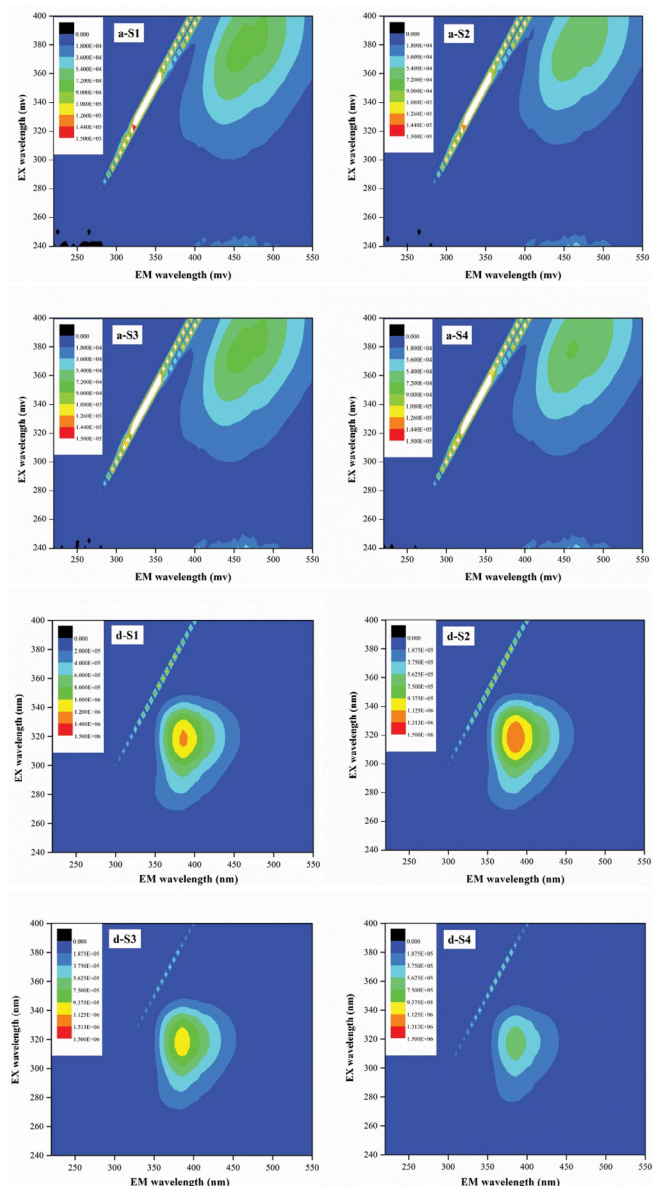


Fig. 8. EEM fluorescence spectra of soluble EPS fractions before and after treatment by steel with different particle size distributions ( $S_1, S_2, S_3$  and  $S_4$ ).

decreased with particle size. Meanwhile, the surface charge of the flocs decreased with S-EPS content, and this change was consistent with that of the zeta potential.

3.2.5. Microstructure

As shown in Fig. 9., the original sludge had a compact layered structure with dense flocs. The inorganic mineral was encapsulated by large numbers of organic substances in the sludge. This compact structure made the sludge highly hydrophilic and difficult to dewater. The RS particles were fine, and strong capillary forces existed between the particles.

The sludge structure noticeably changed, the dense layered structure was destroyed, and numerous granular substances appeared after steel slag conditioning. These

particles had a loose distribution, with large numbers of pores between them, and this structure was conducive to water circulation. Some of the fine particles in the steel slag were insoluble inorganic components and could ensure the outlet channel and provide skeletal support during mechanical dewatering.

### 3.3. Transformation behavior of HMs

Cu, Mn, and Zn content in the filtrate and leaching liquid of the sludge cake was measured to compare the behavior of HMs in the sludge before and after conditioning. The results are shown in Table 6. Cu and Mn concentrations decreased by 60% and 85.2%, respectively, which may be related to the pH increase in the liquid phase. The activity of HMs is negatively correlated with pH, and the stability of metal is improved by alkaline conditions [35]. However,

Zn concentration in the filtrate increased 2.2 times after steel slag conditioning but did not exceed the threshold value prescribed by GB8978-2002. TCLP was performed to identify the leaching characteristics and environmental influence of the RS and conditioned sludge cakes. The results showed that Cu, Mn, and Zn concentrations decreased by 93.5%, 27.1%, and 22.1%, respectively. Thus, the addition of steel slag reduced the risk and enhanced the immobilization of HMs.

The chemical species distribution of HMs can indicate the availability and mobility of HMs. As shown in Fig. 10, Cu was mostly distributed in organic and residual fractions (74.27%) for RS. This result was consistent with the speciation profile of Cu in many previous studies [36]. The percentage of Cu in the organic and residual fractions increased to 78.89% after conditioning possibly because of the increase in pH. The electronegativity of COO<sup>-</sup>, O-H, C=O, and other groups on the surface of organic matter increases with a rise

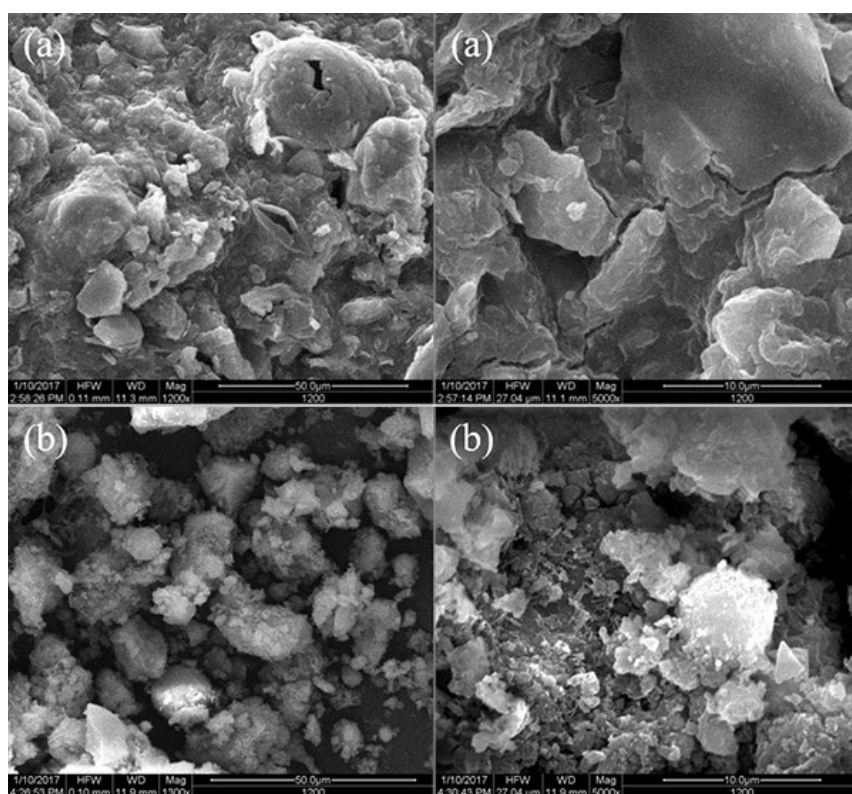


Fig. 9. SEM of raw sludge (a) and sludge conditioned by steel (b).

Table 6  
Concentrations of HMs in the liquid phase TCLP tests (Mean  $\pm$  SD) (mg L<sup>-1</sup>)

	Liquid phase		TCLP tests		Limit value <sup>a</sup>	Limit value <sup>b</sup>
	RS	Conditioned	RS	Conditioned		
Cu	0.005 $\pm$ 0.002	0.002 $\pm$ 0.001	0.52 $\pm$ 0.018	0.0335 $\pm$ 0.011	0.5	40
Mn	0.115 $\pm$ 0.012	0.017 $\pm$ 0.002	13.92 $\pm$ 1.017	10.15 $\pm$ 0.988	2	100
Zn	0.026 $\pm$ 0.003	0.058 $\pm$ 0.007	10.48 $\pm$ 0.111	8.16 $\pm$ 0.105	2	100

<sup>a</sup>Integrated Wastewater Discharge Standard, GB8978–2002, PR China

<sup>b</sup>Standard for Pollution Control on the Landfill Site of Municipal Solid Waste, GB 16889–2008, PR China

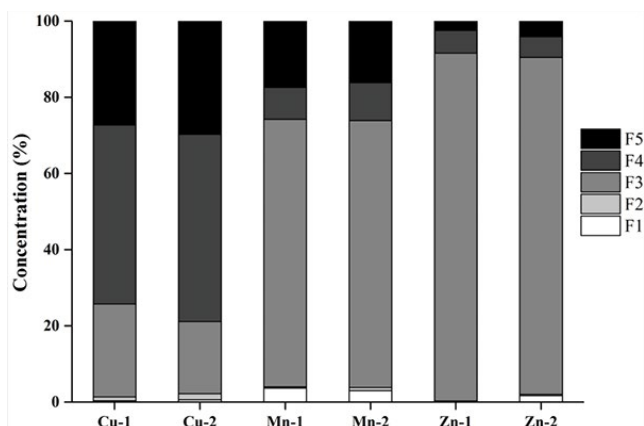


Fig. 10. Fraction distributions of metals in the sludge samples: 1 denotes raw sludge and 2 denotes sludge conditioned by steel.

in pH after dissociation, thereby enhancing the complexation capability of metal ions [37].

In the case of Mn, more than 70% of its compounds were distributed in Fe/Mn-oxide fractions for the RS. The percentage of Mn in the organic and the residual increased from 25.79% to 26.11% after steel slag conditioning. Similar to Mn, Zn was nearly distributed in the Fe/Mn-oxide fraction. The percentage of Fe/Mn-oxide fraction for the RS exceeded 90%, thereby indicating that Mn and Zn were mainly associated with mobile forms. The percentage of Zn in the residual fraction increased from 8.44% to 9.55% after conditioning for the chemical species distribution of HMs. This change confirmed the satisfactory stabilization and low mobility of Zn, and this finding was consistent with the leaching results.

#### 4. Conclusions

The present study revealed that steel slag remarkably improved sludge dewaterability (SRF and CST decreased by 98.8% and 78.6%, respectively) at an optimized conditioning dosage of 40 mg/g DS. Steel slag conditioning decreased the sludge negative charge, decomposed EPS, and induced sludge disintegration. The TCLP tests showed that the Cu, Mn, and Zn concentrations decreased by 93.5%, 27.1%, and 22.1%, respectively. Moreover, analysis of the chemical species distribution demonstrated that the percentage of Cu and Mn in the organic and residual fractions increased by 6.22% and 1.24%, respectively, while the percentage of Zn in the residual fraction increased from 8.44% to 9.55%. These findings indicated that the addition of steel slag could reduce the risk and enhance the immobilization of HMs.

#### Acknowledgments

The authors would like to appreciate the National Key R&D Program of China (No. 2018YFC1801705), the Special Fund of Chinese Central Government for Basic Scientific Research Operations in Commonwealth Research Institutes (No. CKSF2017009/YT), the Special Fund of Chinese Central Government for Basic Scientific Research Operations in Commonwealth Research Institutes (No. CKSF2019168/YT and CKSF2017009/YT).

#### Authors contributions

Conceptualization, Haobo Hou; Data curation, Yuchi Chen, Yiqie Dong, Fucai Huang, Teng Luo and Yun Zheng; Project administration, Haobo Hou; Writing – original draft, Sha Wan and Min Zhou; Writing – review & editing, Sha Wan and Yi Han.

#### References

- [1] L. Hei, C.C. Lee, H. Wang, X.Y. Lin, X.H. Chen, Q.T. Wu, Using a high biomass plant *Pennisetum hybridum* to phyto-treat fresh municipal sewage sludge, *Bioresour. Technol.*, 217 (2016) 252–256.
- [2] E.E. Kwon, T. Lee, Y.S. Ok, D.C.W. Tsang, C. Park, J. Lee, Effects of calcium carbonate on pyrolysis of sewage sludge, *Energy*, 153 (2018) 726–731.
- [3] G. Zhen, X. Lu, L. Su, T. Kobayashi, G. Kumar, T. Zhou, K. Xu, Y.Y. Li, X. Zhu, Y. Zhao, Unraveling the catalyzing behaviors of different iron species (Fe(2+) vs. Fe(0)) in activating persulfate-based oxidation process with implications to waste activated sludge dewaterability, *Water Res.*, 134 (2018) 101–114.
- [4] S. Tao, J. Yang, H. Hou, S. Liang, K. Xiao, J. Qiu, J. Hu, B. Liu, W. Yu, H. Deng, Enhanced sludge dewatering via homogeneous and heterogeneous Fenton reactions initiated by Fe-rich biochar derived from sludge, *Chem. Eng. J.*, 372 (2019) 966–977.
- [5] J. Liu, Q. Yang, D. Wang, X. Li, Y. Zhong, X. Li, Y. Deng, L. Wang, K. Yi, G. Zeng, Enhanced dewaterability of waste activated sludge by Fe(II)-activated peroxymonosulfate oxidation, *Bioresour. Technol.*, 206 (2016) 134–140.
- [6] L.-F. Wang, D.-Q. He, Z.-H. Tong, W.-W. Li, H.-Q. Yu, Characterization of dewatering process of activated sludge assisted by cationic surfactants, *Biochem. Eng. J.*, 91 (2014) 174–178.
- [7] K. Hu, J.Q. Jiang, Q.L. Zhao, D.J. Lee, K. Wang, W. Qiu, Conditioning of wastewater sludge using freezing and thawing: role of curing, *Water Res.*, 45 (2011) 5969–5976.
- [8] A. Mahmoud, J. Olivier, J. Vaxelaire, A.F. Hoadley, Electrical field: a historical review of its application and contributions in wastewater sludge dewatering, *Water Res.*, 44 (2010) 2381–2407.
- [9] L. Huan, J. Yiyang, R.B. Mahar, W. Zhiyu, N. Yongfeng, Effects of ultrasonic disintegration on sludge microbial activity and dewaterability, *J. Hazard. Mater.*, 161 (2009) 1421–1426.
- [10] S. Jomaa, A. Shanableh, W. Khalil, B. Trebilco, Hydrothermal decomposition and oxidation of the organic component of municipal and industrial waste products, *Adv. Environ. Res.*, 7 (2003) 647–653.
- [11] B.B. Wang, X.T. Liu, J.M. Chen, D.C. Peng, F. He, Composition and functional group characterization of extracellular polymeric substances (EPS) in activated sludge: the impacts of polymerization degree of proteinaceous substrates, *Water Res.*, 129 (2018) 133–142.
- [12] G.H. Yu, P.J. He, L.M. Shao, P.P. He, Stratification structure of sludge flocs with implications to dewaterability, *Environ. Sci. Technol.*, 42 (2008) 7944–7949.
- [13] W. Zhang, P. Xiao, Y. Liu, S. Xu, F. Xiao, D. Wang, C.W.K. Chow, Understanding the impact of chemical conditioning with inorganic polymer flocculants on soluble extracellular polymeric substances in relation to the sludge dewaterability, *Sep. Purif. Technol.*, 132 (2014) 430–437.
- [14] Y. Lv, K. Xiao, J. Yang, Y. Zhu, K. Pei, W. Yu, S. Tao, H. Wang, S. Liang, H. Hou, B. Liu, J. Hu, Correlation between oxidation-reduction potential values and sludge dewaterability during pre-oxidation, *Water Res.*, 155 (2019) 96–105.
- [15] Y. Shi, J. Yang, W. Yu, S. Zhang, S. Liang, J. Song, Q. Xu, N. Ye, S. He, C. Yang, J. Hu, Synergetic conditioning of sewage sludge via Fe<sup>2+</sup>/persulfate and skeleton builder: effect on sludge characteristics and dewaterability, *Chem. Eng. J.*, 270 (2015) 572–581.
- [16] J. Song, J. Yang, S. Liang, Y. Shi, W. Yu, C. Li, X. Xu, J. Xiao, R. Guan, N. Ye, X. Wu, H. Hou, J. Hu, J. Hu, B. Xiao, Red mud enhanced hydrogen production from pyrolysis of deep-dewatered sludge

- cakes conditioned with Fenton's reagent and red mud, *Int. J. Hydrogen Energy*, 41 (2016) 16762–16771.
- [17] H. Liu, J. Yang, Y. Shi, Y. Li, S. He, C. Yang, H. Yao, Conditioning of sewage sludge by Fenton's reagent combined with skeleton builders, *Chemosphere*, 88 (2012) 235–239.
- [18] K.B. Thapa, Y. Qi, A.F.A. Hoadley, Interaction of polyelectrolyte with digested sewage sludge and lignite in sludge dewatering, *Colloids Surf., A*, 334 (2009) 66–73.
- [19] M. Cheng, G. Zeng, D. Huang, C. Lai, P. Xu, C. Zhang, Y. Liu, J. Wan, X. Gong, Y. Zhu, Degradation of atrazine by a novel Fenton-like process and assessment the influence on the treated soil, *J. Hazard. Mater.*, 312 (2016) 184–191.
- [20] H. Yi, G. Xu, H. Cheng, J. Wang, Y. Wan, H. Chen, An overview of utilization of steel slag, *Procedia Environ. Sci.*, 16 (2012) 791–801.
- [21] I. Blanco, P. Molle, L.E. Saenz de Miera, G. Ansola, Basic oxygen furnace steel slag aggregates for phosphorus treatment. Evaluation of its potential use as a substrate in constructed wetlands, *Water Res.*, 89 (2016) 355–365.
- [22] Y. Xue, H. Hou, S. Zhu, Adsorption removal of reactive dyes from aqueous solution by modified basic oxygen furnace slag: Isotherm and kinetic study, *Chem. Eng. J.*, 147 (2009) 272–279.
- [23] X. Zhu, F. Li, J. Zhang, S. Wu, Physicochemical properties of stabilized sewage sludge admixtures by modified steel slag, *Open Chem.*, 16 (2018) 583–590.
- [24] C. Vogel, C. Adam, Heavy metal removal from sewage sludge ash by thermochemical treatment with gaseous hydrochloric acid, *Environ. Sci. Technol.*, 45 (2011) 7445–7450.
- [25] G.C. Cotzias, Manganese in health and disease, *Phys. Rev.*, 38 (1958) 503–532.
- [26] X. Wang, C. Li, B. Zhang, J. Lin, Q. Chi, Y. Wang, Migration and risk assessment of heavy metals in sewage sludge during hydrothermal treatment combined with pyrolysis, *Bioresour. Technol.*, 221 (2016) 560–567.
- [27] Q. Xu, Q. Wang, W. Zhang, P. Yang, Y. Du, D. Wang, Highly effective enhancement of waste activated sludge dewaterability by altering proteins properties using methanol solution coupled with inorganic coagulants, *Water Res.*, 138 (2018) 181–191.
- [28] H. Wei, J. Ren, A. Li, H. Yang, Sludge dewaterability of a starch-based flocculant and its combined usage with ferric chloride, *Chem. Eng. J.*, 349 (2018) 737–747.
- [29] A. Tessier, P.G.C. Campbell, M. Bisson, Sequential extraction procedure for the speciation of particulate trace-metals, *Anal. Chem.*, 51 (1979) 844–851.
- [30] Y. Han, M. Zhou, Y.H. Xiao, X. Zhou, J.J. Geng, T. Wang, S. Wan, H.B. Hou, Roles of Fe(III) and Fe(VI) in enhancing dewaterability of sewage sludge based on floc size grading, *Desal. Wat. Treat.*, 84 (2017) 324–331.
- [31] Y.h. Yang, D.h. Zhang, Concentration effect on the fluorescence spectra of humic substances, *Commun. Soil Sci. Plant Anal.*, 26 (2008) 2333–2349.
- [32] Z. Wang, Z. Wu, S. Tang, Characterization of dissolved organic matter in a submerged membrane bioreactor by using three-dimensional excitation and emission matrix fluorescence spectroscopy, *Water Res.*, 43 (2009) 1533–1540.
- [33] G. Zhen, X. Lu, Y. Li, Y. Zhao, B. Wang, Y. Song, X. Chai, D. Niu, X. Cao, Novel insights into enhanced dewaterability of waste activated sludge by Fe(II)-activated persulfate oxidation, *Bioresour. Technol.*, 119 (2012) 7–14.
- [34] Y. Yamashita, E. Tanoue, Chemical characterization of protein-like fluorophores in DOM in relation to aromatic amino acids, *Marine Chem.*, 82 (2003) 255–271.
- [35] G. Merrington, I. Oliver, R.J. Smernik, M.J. McLaughlin, The influence of sewage sludge properties on sludge-borne metal availability, *Adv. Environ. Res.*, 8 (2003) 21–36.
- [36] A. Fuentes, M. Llorens, J. Saez, M.A. Isabel Aguilar, J.F. Ortuno, V.F. Meseguer, Comparative study of six different sludges by sequential speciation of heavy metals, *Bioresour. Technol.*, 99 (2008) 517–525.
- [37] A.E. Boekhold, E.J.M. Temminghoff, S.E.A.T.M. Vanderzee, Influence of electrolyte-composition and pH on cadmium sorption by an acid sandy soil, *J. Soil Sci.*, 44 (1993) 749–749.